4^{th} *URSI AT-RASC, Gran Canaria, 19 – 24 May 2024*

High Directional Fabry-Perot Millimeter-wave Antenna for D-band Spectrum

Rana Muhammad Hasan Bilal(1), Michele Borgese(2), Simone Genovesi(1),Giuliano Manara(1), and Filippo Costa(1)
(1) Department of Information Engineering, University of Pisa 56125, Italy.
(2) Research and Development Department, SIAE Microelettronica, Cologno Monzese, Italy.

Abstract

This paper investigates a low-profile, low-cost and high gain D-band Fabry-Perot (FP) antenna for millimeter-wave (mm-wave) applications. The geometric configuration of the antenna comprises with a top partially reflective surface (PRS) which is mounted over a metal-coated dielectric substrate. The standard rectangular waveguide (WR5) is employed below the ground-plane to excite the antenna. The proposed D-band FP antenna shows a maximum gain of 16 dBi at 151.2 GHz with a good impedance matching with an S_{11} value of -12 dB. The impedance matching is achieved by employing a pair of rectangular strips along the left and right edges of slotted ground-plane. Moreover, the total efficiency of this D-band FP antenna is around 60%. This type of high-gain antenna holds potential applications in high-frequency mm-wave spectrum, including remote sensing and radar systems.

1 Introduction

The mm-wave spectrum which contains the operating frequencies from 30 GHz to 300 GHz, gaining a significant attention in various applications namely antennas, high-frequency circuits, and integrated mm-wave and terahertz (THz) devices [1–3]. The upcoming sixth-generation (6G) technology has achieved the interest of researchers owing to its prominent role in mm-wave and sub-THz communication systems [4]. The mm-wave band contains high frequencies and it attracts the research community owing to its demand in a series of important applications including, remote sensing, automotive radars, astronomy, medical imaging, and advanced wireless communication systems etc [5].

High-directional antennas play a pivotal role in mm-wave applications and they minimize the propagation losses in a long-range communications. FP antennas have become popular due to the advancements in wireless communication systems and the increasing demand for high-gain in the high-frequency mm-wave spectrum [6]. FP antennas have attracted significant attention in recent years due to their advantages, such as high gain, low profile, simple structure, and cost-effectiveness, making them a suitable candidate over bulky horns or corporate-fed arrays. The application of FP antenna technologies has extended to the mm-wave band and they can be implemented by employing band-gap (BG) structures, periodic PRS, single-layer dielectric superstrates, and frequency-selective surfaces (FSS). The main advantage of using a FP antenna is to realize an increased gain and it also provides an efficient and cost-effective fabrication [7]. The geometrical layout of the standard FP antenna comprises with an input source, a ground plane, and a PRS placed at a $\lambda/2$ distance from the ground plane which forms an air-filled cavity [8].

Other types of FP antenna structures have been implemented using different design methodologies, including the utilization of single and multilayered PRS to achieve wideband [9–14], dielectric superstrates [15, 16], shaped ground planes [17], and conical short horns [18]. Most of the available FP antennas operate in microwave frequencies. Some mm-wave FP antennas are also reported in the literature, typically implemented with a single-layer configuration of PRS. For instance, a 30 GHz FP antenna is presented in [19] employed PRS to enhance the gain by 8.5 dB. Moreover, numerous FP antennas have been specifically designed for 60 GHz or 90 GHz, employing a single-layer dielectric PRS [20] and dual-layer dielectric PRS [21–23]. In reference [20], a single substrate with coaxial probe feeding has been utilized by cutting the ground-plane, whereas in references [21–23], they employed a dual-layer of dielectric substrates to achieve the desired level of gain. Typically, within FP antennas, radiation bounces back and forth between the upper PRS and the lower ground-plane of the dielectric cavity. When a fraction of the radiation reaches beyond the cavity, it creates an in-phase superposition, leading to an enhanced directivity along the boresight direction [24, 25].

In this article, the authors aim to design a FP antenna for high-frequency mm-wave band, with a specific focus on the D-band. The proposed D-band FP antenna consists of a single block of a thin dielectric (ITERA MT40) where an array of inductive grids serving as a PRS is etched on the top side. To excite the antenna, a WR5 rectangular waveguide is employed as the input source, with an operating frequency range spanning from 140 to 220 GHz. The waveguide is connected to the bottom side of the dielectric layer through an aperture which is opportunely designed to achieve impedance matching. The proposed D-band FP antenna exhibits resonance at 151.2 GHz and achieves a gain of 16 dBi. Due to the simplicity, low-cost and compactness, the proposed high-gain antenna holds potential applications in high-frequency mm-wave scenarios, including radar systems and remote sensing applications.

2 Design of a FP antenna

The geometric layout of the proposed D-band FP antenna is highlighted in Fig. 1. It composes of a top FSS which serves as a PRS and they are grown over a dielectric substrate made of ITERA MT40 (ε_r = 3.38, $\tan\delta$ = 0.0027).

The thickness of the dielectric substrate is selected as 0.5 mm which corresponds to a half-wavelength at the antenna operating frequency. The top PRS and bottom ground-plane are made of metallic copper having thickness of 0.035 mm.

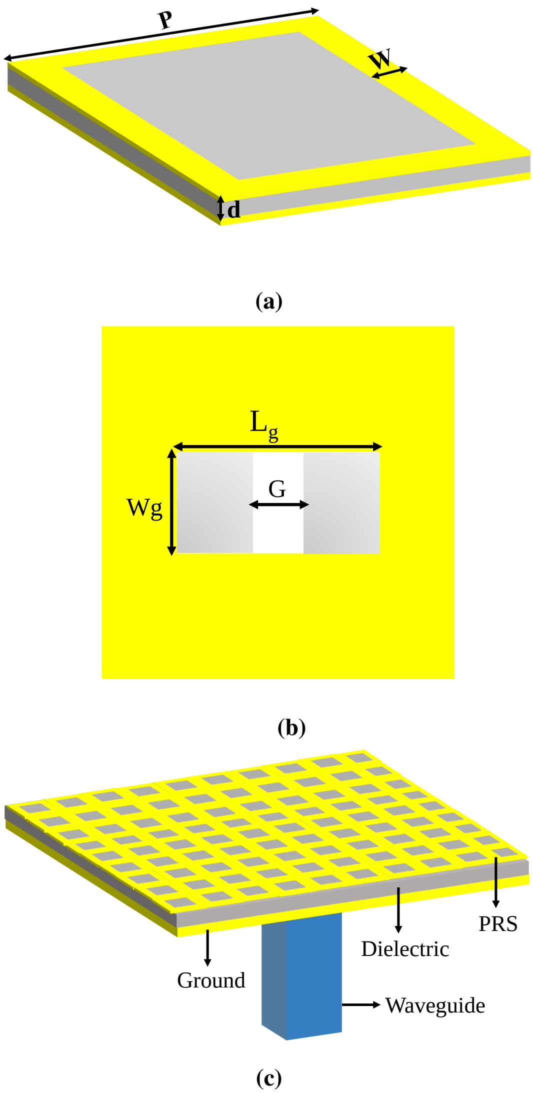

Figure 1. Geometric layout of the proposed D-band FP antenna, comprising a total of 32×32 unit cells (a) Side view of the unit cell featuring a three layers device configuration with top and bottom layers of copper and a middle dielectric spacer, where P = 0.55 mm, W = 0.11 mm and d = 0.5 mm (b) Bottom view of the proposed D-band FP antenna showcasing a pair of rectangular strips for single waveguide source excitation and (c) Side view of periodic arrays of PRS showcasing a unit cell array. This depiction illustrates a periodic surface with a 10×9 unit cell configuration as an example.

The total size of the antenna is selected as 17.6 mm × 17.6 mm (32×32 unit cells). The length and width of each contributing inductive grid are optimized as 0.55 mm and 0.11 mm respectively. For the excitation purposes, a WR5 rectangular waveguide is employed

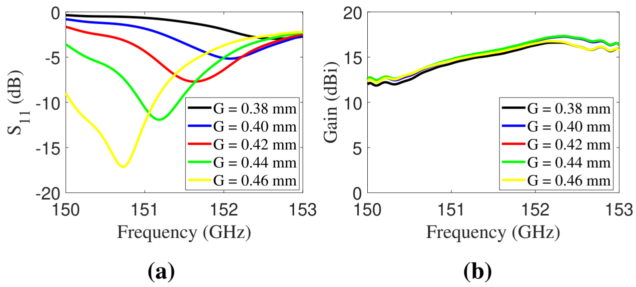

Figure 2. Performance analysis of the proposed D-band FP antenna with a variation of gap (G) (a) The trend of S_{11} parameter of the proposed D-band FP antenna under the variation of different values of the parameter G, and (b) The trend of maximum gain of the proposed D-band FP antenna under the variation of different values of the parameter G.

below the ground-plane. The corresponding length (L_g) and (W_g) of this waveguide are 1.3 mm and 0.65 mm respectively, as described in Fig. 1b. The entire modeling and simulation performance of the proposed D-band FP antenna are characterized by using CST studio software.

3 Results and discussion

In this section, the performance analysis of the proposed D-band FP antenna has been discussed. Initially, the impedance matching characteristics of the designed antenna is described in section 3.1. Thereafter, the key parameters of the proposed antenna including gain, efficiency and S_{11} have been explained in next section 3.2.

3.1 Impedance matching

To achieve the required impedance matching condition of the proposed D-band FP antenna, a pair of rectangular strips is used beneath the ground-plane. The gap (G) between the two strips which is a key parameter to achieve the desired impedance matching condition at the required frequency point. When the gap (G) varies, it significantly affects the S_{11} parameter of the proposed FP antenna while keeping the gain fixed.

Fig. 2 illustrates the variation in the S_{11} parameter and gain as we adjust the value of G within the range of 0.38 mm to 0.46 mm, with an increment of 0.02 mm. Fig. 2a clearly demonstrates that as G increases, the S_{11} shifts towards lower operating frequencies, accompanied by a decrease in magnitude of S_{11}. Ultimately, at G = 0.44 mm, the proposed FP antenna exhibits good impedance matching and shows an S_{11} value of -12 dB at 151.2 GHz. Furthermore, the suggested D-band FP antenna demonstrates a nearly identical gain pattern when varying the parameter G from 0.38 mm to 0.46 mm in 0.02 mm increments, as presented in Fig. 2b. It achieves a peak gain of approximately 16 dBi at 151.2 GHz across all the values of G.

3.2 Radiation performance

To achieve the maximum gain from the proposed D-band FP antenna, an arrangement of 32×32 unit cells, compris-

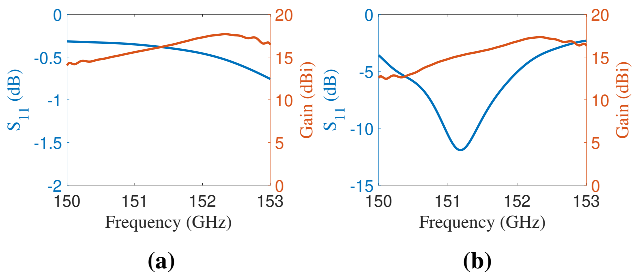

Figure 3. Performance of the proposed D-band FP antenna with and without the matching strips. (a) Maximum gain and S_{11} without rectangular strips and (b) Maximum gain and S_{11} with rectangular strips.

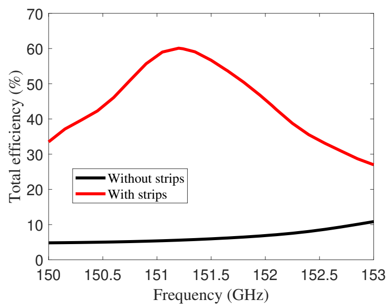

Figure 4. Comparative analysis of the total efficiency of the proposed D-band FP antenna with and without matching strips.

ing inductive grids, is printed on a dielectric substrate, serving as a PRS. In Fig. 3, a comparative analysis of the performance of the proposed D-band FP antenna is presented by analyzing on its maximum gain and S_{11} parameter with and without the matching strips. Initially, we examine the scenario where no rectangular strips are used along the left and right edges of the slotted ground-plane, as illustrated in Fig. 3a. From Fig. 3a, it is evident that the proposed antenna is not radiating efficiently and this is attributed to the impedance mismatch between the input source and the top PRS. Nevertheless, it achieves a maximum gain of 16 dBi. On the contrary, Fig. 3b illustrates the same trend of the gain over a large frequency spectrum but it shows a good impedance matching with an S_{11} value of -12 dB at 151.2 GHz. This impedance matching is achieved by employing a pair of rectangular strips along the left and right edges of the slotted ground-plane.

Fig. 4 provides a comparison of the overall efficiencies between two configurations: one without rectangular strips and the other with rectangular strips. As depicted in Fig. 4, the proposed D-band FP antenna achieves a total efficiency of 60 %, when a pair of rectangular strips is incorporated beneath the slotted ground-plane. Conversely, the configuration without a pair of rectangular strips demonstrates a lower efficiency, approximately 6 %.

4 Conclusion

A mm-wave Fabry-Perot antenna operating in the D-band has been designed. The proposed FP antenna consists of a single block of dielectric (ITERA MT40), which is etched on the top side to obtain an array of 32×32 unit cells of inductive grid, served as a PRS. The bottom surface of the dielectric features a metallic layer with the combination of waveguide aperture, where metallic strips are vertically placed and optimized to achieve impedance matching. The key parameters of the proposed FP antenna such as gain, S_{11}, and efficiency were taken into account to briefly study the performance. The antenna demonstrated a maximum gain of 16 dBi and an efficiency of 60%.

References

[1] X. Wang, L. Kong, F. Kong, F. Qiu, M. Xia, S. Arnon, and G. Chen, "Millimeter wave communication: A comprehensive survey," *IEEE Communications Surveys & Tutorials*, vol. 20, no. 3, pp. 1616–1653, 2018.

[2] N. Al-Falahy and O. Y. Alani, "Millimetre wave frequency band as a candidate spectrum for 5g network architecture: A survey," *Physical Communication*, vol. 32, pp. 120–144, 2019.

[3] B. Heydari, M. Bohsali, E. Adabi, and A. M. Niknejad, "Millimeter-wave devices and circuit blocks up to 104 ghz in 90 nm cmos," *IEEE Journal of Solid-State Circuits*, vol. 42, no. 12, pp. 2893–2903, 2007.

[4] W. Hong, Z. H. Jiang, C. Yu, D. Hou, H. Wang, C. Guo, Y. Hu, L. Kuai, Y. Yu, Z. Jiang *et al.*, "The role of millimeter-wave technologies in 5g/6g wireless communications," *IEEE Journal of Microwaves*, vol. 1, no. 1, pp. 101–122, 2021.

[5] T. E. Bogale, X. Wang, and L. B. Le, "mmwave communication enabling techniques for 5g wireless systems: A link level perspective," in *MmWave Massive MIMO*. Elsevier, 2017, pp. 195–225.

[6] H. Attia, M. L. Abdelghani, and T. A. Denidni, "Wideband and high-gain millimeter-wave antenna based on fss fabry–perot cavity," *IEEE transactions on antennas and propagation*, vol. 65, no. 10, pp. 5589–5594, 2017.

[7] Q.-Y. Guo and H. Wong, "Wideband and high-gain fabry–pérot cavity antenna with switched beams for millimeter-wave applications," *IEEE Transactions on Antennas and Propagation*, vol. 67, no. 7, pp. 4339–4347, 2019.

[8] F. Costa, D. Bianchi, A. Monorchio, and G. Manara, "Linear fabry-perot/leaky-wave antennas excited by multiple sources," *IEEE Transactions on Antennas and Propagation*, vol. 66, no. 10, pp. 5150–5159, 2018.

[9] Y. Ge, K. P. Esselle, and T. S. Bird, "The use of simple thin partially reflective surfaces with positive reflection phase gradients to design wideband, low-profile ebg resonator antennas," *IEEE Transactions on Antennas and Propagation*, vol. 60, no. 2, pp. 743–750, 2011.

[10] Z. Liu, W. Zhang, D. Fu, Y. Gu, and Z. Ge, "Broadband fabry-perot resonator printed antennas using fss superstrate with dissimilar size," *Microwave and Optical Technology Letters*, vol. 50, no. 6, pp. 1623–1627, 2008.

[11] P.-Y. Qin, L.-Y. Ji, S.-L. Chen, and Y. J. Guo, "Dual-polarized wideband fabry–pérot antenna with quad-layer partially reflective surface," *IEEE Antennas and Wireless Propagation Letters*, vol. 17, no. 4, pp. 551–554, 2018.

[12] Y. Ge, C. Wang, and X. Zeng, "Design of a compact wideband high-gain mmw antenna based on fabry-perot antenna concept," in *2014 IEEE Antennas and Propagation Society International Symposium (APSURSI)*. IEEE, 2014, pp. 448–449.

[13] M. W. Niaz, Y. Yin, R. A. Bhatti, Y.-M. Cai, and J. Chen, "Wideband fabry–perot resonator antenna employing multilayer partially reflective surface," *IEEE Transactions on Antennas and Propagation*, vol. 69, no. 4, pp. 2404–2409, 2020.

[14] X. Liu, Z. Yan, E. Wang, T. Zhang, and F. Fan, "Magnetoelectric dipole-fed fabry–perot antenna with wideband rcs reduction based on multilayer metasurface," *IEEE Antennas and Wireless Propagation Letters*, vol. 20, no. 7, pp. 1342–1346, 2021.

[15] R. M. Hashmi, B. A. Zeb, and K. P. Esselle, "Wideband high-gain ebg resonator antennas with small footprints and all-dielectric superstructures," *IEEE Transactions on Antennas and Propagation*, vol. 62, no. 6, pp. 2970–2977, 2014.

[16] N. Wang, L. Talbi, Q. Zeng, and J. Xu, "Wideband fabry-perot resonator antenna with electrically thin dielectric superstrates," *IEEE Access*, vol. 6, pp. 14 966–14 973, 2018.

[17] L.-Y. Ji, P.-Y. Qin, and Y. J. Guo, "Wideband fabry-perot cavity antenna with a shaped ground plane," *IEEE Access*, vol. 6, pp. 2291–2297, 2017.

[18] Y. Ge, Z. Sun, Z. Chen, and Y.-Y. Chen, "A high-gain wideband low-profile fabry–pérot resonator antenna with a conical short horn," *IEEE Antennas and wireless propagation letters*, vol. 15, pp. 1889–1892, 2016.

[19] M. Akbari, S. Gupta, M. Farahani, A. Sebak, and T. Denidni, "Gain enhancement of circularly polarized dielectric resonator antenna based on fss superstrate for mmw applications," *IEEE Transactions on antennas and Propagation*, vol. 64, no. 12, pp. 5542–5546, 2016.

[20] A. Hosseini, F. De Flaviis, and F. Capolino, "A 60 ghz simple-to-fabricate single-layer planar fabry–pérot cavity antenna," *IET Microwaves, Antennas & Propagation*, vol. 9, no. 4, pp. 313–318, 2015.

[21] A. Hosseini, F. Capolino, and F. De Flaviis, "Gain enhancement of a v-band antenna using a fabry-perot cavity with a self-sustained all-metal cap with fss," *IEEE Transactions on Antennas and Propagation*, vol. 63, no. 3, pp. 909–921, 2014.

[22] H. Vettikalladi, O. Lafond, and M. Himdi, "High-efficient and high-gain superstrate antenna for 60-ghz indoor communication," *IEEE Antennas and Wireless Propagation Letters*, vol. 8, pp. 1422–1425, 2009.

[23] K. Konstantinidis, A. P. Feresidis, P. S. Hall, and M. J. Lancaster, "Design of fabry-perot cavity antenna at 94 ghz," in *2012 Loughborough Antennas & Propagation Conference (LAPC)*. IEEE, 2012, pp. 1–4.

[24] Y.-H. Lv, X. Ding, and B.-Z. Wang, "Dual-wideband high-gain fabry-perot cavity antenna," *IEEE Access*, vol. 8, pp. 4754–4760, 2019.

[25] F. P. Casares-Miranda, C. Camacho-Peñalosa, and C. Caloz, "High-gain active composite right/left-handed leaky-wave antenna," *IEEE transactions on antennas and propagation*, vol. 54, no. 8, pp. 2292–2300, 2006.